FSI-96-00-1

Three-Dimensional Thixotropic Flow Model

M.R. Barkhudarov, C.L. Bronisz, C.W. Hirt

Flow Science, Inc.
1325 Trinity Drive, Los Alamos, NM 87544

Presented at 4th International Conference on Semi-Solid Processing of Alloys and Composites
19-21 June, 1996, The University of Sheffield, England

ABSTRACT

Advantages of the semi-solid metal forming process over conventional forging and high pressure die casting have generated significant interest in recent years among casting manufacturers. Mathematical and numerical modeling of the behavior of thixotropic materials is crucial to provide understanding of the roles a variety of factors play in the efficiency of the process and the quality of the final product. These factors include, for example, the size of the solid grains in the preformed billet, the initial solid fraction, temperature distribution, ram speed and load, and the mold temperature. The present work describes a simple numerical model of thixotropic behavior that sets up a framework for future development. The approach is based on using the apparent dynamic viscosity, μ. A transport equation for μ includes advection terms and a relaxation term that accounts for the thixotropy of the material. The relaxation term is defined by two variables, the steady-state viscosity, μ_0, and the relaxation time, τ, both of which may be functions of the shear rate and solid fraction and can be defined from empirical data. No yield stress, wall slip and elastic or plastic behavior at high solid fractions is included at this stage. In this form, the model applies to flows with low and medium values of solid fraction, $f_S < 0.6 - 0.7$. The numerical development is based on the general purpose, commercial CFD program FLOW-3D widely used for filling and solidification analysis. It is shown that, despite the simplicity of the mathematical model, experimental measurements for the apparent steady-state viscosity and transient shear stress can be matched with reasonable accuracy. Finally, an extrusion flow is simulated showing that the die swell ratio depends on the thixotropic relaxation time.

1. INTRODUCTION

Over the last 20 years, since the early work of Spencer, *et al* [1972] using an Sn-15%Pb alloy, significant amount of experimental data have been produced on the rheological behavior of Sn-Pb and aluminum based thixotropic alloys. These experiments mainly involved measuring the apparent steady-state viscosity as a function of the shear rate and solid fraction using a variety of methods, most commonly, cylindrical Couette rheometers. Fewer experiments have considered transient thixotropic flows (*e. g.* Joly and Mehrabian [1976] and Kumar, *et al* [1993]). Comprehensive reviews of the experimental, theoretical and technological aspects of thixotropy can be found in Flemings [1991], Kirkwood [1994] and Sigworth [1995].

Transient thixotropic properties are harder to measure than steady-state flow parameters since it is difficult to achieve a flow uniformity with continuously changing flow conditions, such as shear rate and temperature. In addition to time scales associated with particle agglomeration and breakup, there is a viscous diffusion time scale that defines the rate at which fluid momentum diffuses from the moving wall of the rheometer into the metal bulk. For a fluid of density ρ and constant viscosity μ it will take an approximate time of $\tau = \rho L^2/\mu$ to establish a uniform shear rate profile in a Couette flow after one of the moving walls changes its speed (L is the distance between the two walls in the rheometer). If cooling or heating takes place, then thermal diffusion and phase change processes introduce additional time scales needed to establish a uniform temperature and solid fraction distribution. Furthermore, during cooling initially round grains may evolve into dendrites. According to Sigworth [1995], such a transition would lead to a dramatic increase in the apparent viscosity.

It is clear that a mathematical model that describes comprehensively all aspects of the thixotropic rheology is extremely difficult to develop. With that in mind a simple mathematical model that can be easily tuned to fit rheological properties of a particular material, without going into details of the slurry internal structure evolution, appears attractive. Such an approach, called 'engineering modeling,' is outlined in the next section followed by calculated examples.

2. GOVERNING EQUATION

The evolution of the apparent viscosity can be described by the following transport equation:

$$\frac{\partial \mu}{\partial t} + (\mathbf{u}\nabla)\mu = \omega(\mu_0 - \mu) \tag{1}$$

where $\mathbf{u}$ is the fluid velocity, $\mu_0(\dot{\gamma}, f_s)$ the fluid viscosity at constant shear rate and solid fraction and $\tau = 1/\omega$ is a relaxation time. The relaxation time can also be a function of $\dot{\gamma}$ and f_s.

Equation (1) can be directly related to the so-called Moore model in which the internal structure is represented by a single variable λ and the transport equation for λ includes terms describing structural buildup and dissagglomeration (Kirkwood [1994]):

$$\frac{\partial \lambda}{\partial t} + (\mathbf{u}\nabla)\lambda = b_1(1-\lambda) - b_2\lambda\dot{\gamma}, \quad 0 \le \lambda \le 1 \tag{2}$$

where b_1 and b_2 are positive constants. The apparent viscosity is a linear function of λ

$$\mu = \mu_\infty + c\lambda \tag{3}$$

where μ_∞ and c also are positive constants. Substituting Eq. (3) into Eq. (1) yields the correspondence between our model and that of Moore

$$\mu_0 = \mu_\infty + \frac{b_1 c}{b_1 + b_2 \dot{\gamma}} \quad \text{and} \quad \omega = b_1 + b_2 \dot{\gamma} \tag{4}$$

3. HYSTERESIS AND RELAXATION TIME

The amount of thixotropy in an alloy can be characterized by the magnitude of the hysteresis in a cyclic shear-stress versus shear-rate curve. A simple cyclic process can be carried out by increasing the shear rate from rest at a constant rate, $d\dot{\gamma}/dt = a$, to a maximum value, $\dot{\gamma} = \dot{\gamma}_{max}$, then holding the shear constant for a fixed period of time, Δt, and finally reducing $\dot{\gamma}$ back to zero at the same rate, $d\dot{\gamma}/dt = -a$. The area of the hysteresis is

$$\oint \sigma d\dot{\gamma} = \int_0^T \mu \dot{\gamma} \frac{d\dot{\gamma}}{dt} dt \tag{5}$$

where T is the total time of the hysteresis cycle. The area of the hysteresis grows with the maximum shear rate, $\dot{\gamma}_{max}$, since for the same value of a, T in Eq. (5) increases with $\dot{\gamma}_{max}$. The hysteresis is also larger for shorter upward time, *i. e.* larger values of $d\dot{\gamma}/dt$, because viscosity has less time to relax to the steady-state value, $\mu_0(\dot{\gamma})$. A longer rest time prior to the beginning of the shearing cycle will give larger hysteresis because this leads to a larger initial value of μ. Similarly, longer holding times, Δt, will magnify the hysteresis because μ will be smaller at the beginning of the downward part of the shearing cycle. These observations are in agreement with the experimental data given by Joly and Mehrabian [1976].

Using Eq. (1) we can write

$$\frac{d\sigma}{d\dot{\gamma}} = \frac{d}{d\dot{\gamma}}(\mu\dot{\gamma}) = \mu + \dot{\gamma}\frac{d\mu}{d\dot{\gamma}} = \mu + \frac{\dot{\gamma}}{\tau \frac{d\dot{\gamma}}{dt}}(\mu_0 - \mu) \tag{6}$$

The relaxation time then can be calculated as

$$\tau = \frac{\dot{\gamma}(\mu_0 - \mu)}{\frac{d\dot{\gamma}}{dt}\left(\frac{d\sigma}{d\dot{\gamma}} - \mu\right)} \tag{7}$$

Quantities on the right side may be evaluated using experimental hysteresis curves shown in Fig. 1*a*. These curves were obtained for Sn-15%Pb alloy at $f_s = 0.45$ by Joly and Mehrabian [1976]. The upward time was 2 *s* and $\dot{\gamma}_{max} = 115\ s^{-1}$. The four curves were obtained for four values of the rest time prior to shearing, t_r=0.5 *min*, 2 *min*, 7.5 *min* and 30 *min.*

For the steady-state viscosity we assume

$$\mu_0(\dot{\gamma}) = \mu_\infty \left[1 + \left(\frac{\dot{\gamma}^*}{\dot{\gamma}} \right)^2 \right]^{0.465} \tag{8}$$

where $\mu_\infty = 0.05\ Nsm^{-2}$ and $\dot{\gamma}^* = 1880\ s^{-1}$ as derived from the data given in Fig. 2. Equation (8) appears more siutable to fit the experimental data, than Eq. (4). Figure 3 shows plots of the relaxation time versus shear rate derived from the upward parts of the hysteresis curves in Fig. 1*a* for $10 < \dot{\gamma} < 100$. It can be seen that the relaxation times for $t_r = 0.5\ min$ and $t_r = 7.5\ min$ (denoted $\tau_{0.5}$ and $\tau_{7.5}$, respectively) are remarkably close at all shear rates except for $\dot{\gamma} = 50\ s^{-1}$, where $\tau_{7.5}$ exceeds $\tau_{0.5}$ by a factor of two. However, relaxation times for the other two cases, τ_2 and τ_{30}, are not that close. This could partially be explained by the uncertainties in the experimental measurements of the shear stress versus shear rate behavior.

At $\dot{\gamma} = 0$ τ can be evaluated from the difference in the rest times and slopes of the four curves in Fig.1*a*. This estimate shows that $\tau(0) \sim 60\ s$, indicating that the curves in Fig. 3 should steeply go up as shear rate approaches zero. The steep decrease of the relaxation time as the shear rate increases from zero may be explained by a breakdown of internal structure that builds up at rest. Due to the lack of resolution in the experimental curves, it is difficult to compute τ directly from Eq. (7) at small shear rates, $\dot{\gamma} < 10$. Therefore, the following expression was assumed for the relaxation time at $\dot{\gamma} < 10$

$$\tau = a_1 e^{-(\dot{\gamma}/\dot{\gamma}_0)^{a_2}} \tag{9}$$

where $a_1 = 60\ s$, and a_2 and $\dot{\gamma}_0$ are chosen to match the value and the approximate slope of one of the $\tau(\dot{\gamma})$ curves at $\dot{\gamma} = 10\ s^{-1}$ in Fig. 3. Numerical tests showed that results are not overly sensitive to the values of $\dot{\gamma}_0$ and a_2 in Eq. (9).

A fully three-dimensional numerical implementation of Eq. (1) is based on a general purpose control volume CFD package FLOW-3D widely used for casting analysis (Sicilian, *et al* [1987]). An implicit algorithm is employed to approximate viscous terms in the Navier-Stokes equations to avoid time step size stability limitations. Viscosity μ in the source term on the right side of Eq. (1) is also approximated implicitly. The resulting algebraic equation is easily solved for μ since the source term is linear.

A planar Couette flow was considered with the shearing cycle parameters $a = 57.5\ s^{-2}$ and $\dot{\gamma}_{max} = 115\ s^{-1}$. Only the upward segment of the hysteresis was modeled because, firstly, it is the most interesting and difficult to match that part of the experiment and, secondly, the exact parameters of the holding and downward periods were not given in the original publication by Joly and Mehrabian [1976]. A constant time step of $0.0005\ s$ was used in the simulations.

Within the framework of the present approach, a variation in t_r results in a different initial value of the apparent viscosity, $\mu_{t=0}$. An estimate using data in Fig. 1*a* gave approximate initial values of the viscosity for the four cases as

$\mu_{0.5} = 22.0\ Nsm^{-2}$, $\mu_{2.0} = 45.0\ Nsm^{-2}$, $\mu_{7.5} = 60.0\ Nsm^{-2}$ and $\mu_{30} = 75.0\ Nsm^{-2}$.

First, the relaxation time was taken to be piece-wise linear according to the $\tau_{7.5}$ curve in Fig. 3 (long-dash line). In this case in Eq. (9)

$$a_2 = 0.18 \quad \text{and} \quad \dot{\gamma}_0 = 1.56 \times 10^{-3}\ s^{-1} \tag{10}$$

Computed shear stresses and apparent viscosities for the four initial values of μ are plotted versus time for $0 < t < 2\ s$ in Figs. 4*a* and 4*b*. The stress results are similar to those in Fig. 1*a*. The shear stress in each case increases steeply at the beginning of shearing since the apparent viscosity is still large. However, as the steady-state viscosity decreases and the relaxation time drops below 0.5 *s*, the apparent viscosity decreases rapidly producing a small plateau in the stress curve at $t \approx \tau$. As μ continues to drop so does the stress. The decrease of the viscosity then slows down as τ starts to grow at $t > 0.5\ s$ ($\dot{\gamma} > 30\ s^{-1}$). This results in another plateau in the stress curve at $t \approx 1\ s$. Viscosity continues to drop after that but at a slower rate and the stress increases again until the shear rate reaches the maximum, $\dot{\gamma} = \dot{\gamma}_{max}$, at $t = 2\ s$.

The maximum shear stress at the first plateau is somewhat overestimated in the numerical predictions, more so for larger initial viscosities (or rest times). The experimental curve for $t_r = 30\ min$ does not even have a maximum at this point. However, the results at later times correspond to the experiment more accurately.

The second series of stress curves, Figs. 4*c* and 4*d*, were obtained using the $\tau_{0.5}$ curve in Fig. 3 (solid line). The same coefficients in Eq. (9) were employed (Eq. (10)). It is interesting that, despite obvious similarities in the $\tau_{0.5}$ and $\tau_{7.5}$ curves, stress values in Figs. 4*a* and 4*c* with the same initial viscosity are quite different for $t > 0.7\ s$. In fact, results in Fig. 4*c* are more similar to the experimental curves shown in Fig. 1*b* which were obtained at a solid fraction just 5% below that used in Fig. 1*a*, $f_s = 0.4$.

5. DIE SWELL PHENOMENON

The thixotropic model was used to simulate die swell phenomena during extrusion (Richardson [1970]). The material was assumed to be an Sn-Pb alloy at a solid fraction of 0.45 and initial apparent viscosity of 30 $Ns\ m^{-2}$. The cylindrical nozzle through which the metal was extruded had a diameter of D_0=5 *mm* and length of l=5 *mm*. The average extrusion velocity in the nozzle was around U=0.09 *m/s* corresponding to a shear rate of approximately 50 s^{-1}. The influence of the relaxation time on swelling was investigated. Swelling occurs due to a relaxation from the boundary layer flow inside the nozzle to a free stream flow outside the nozzle, and is usually characterized by a swelling ratio, D/D_0, where D is the diameter of the free flow stream. The swelling ratio depends on the amount of adjustment occurring in the emerging flow and on the rate of this adjustment.

Three constant relaxation times were used in the simulations: *a*) 0 *s*; *b*) 0.05 *s*; *c*) 10.0 *s*. The first case corresponds to a Non-Newtonian fluid with no thixotropy, *i. e.* the apparent viscosity in the flow is defined by the instantaneous value of the local shear rate and has no time dependence. Therefore, flow adjustment occurs immediately after the metal emerges from the nozzle (Fig. 5*a*). No swelling is observed in this case because the viscous boundary layer inside the nozzle is thin with the apparent viscosity near walls decreasing to $0.7\ Ns\ m^{-2}$. The flow in the middle of the nozzle is near uniform ('plug flow') and little adjustment is needed to achieve a uniform velocity profile outside the nozzle. Swelling ratios of 1.37 and 1.27 are observed in cases *b*) and *c*), respectively, Figs. 5*b* and 5*c*. Because of non-zero relaxation times in these cases, viscosity does not decrease due to shearing as much as in case *a*). Therefore, essentially non-uniform velocity profiles develop across the entire nozzle diameter, leading to substantial swelling. It appears that the largest swelling is achieved in case *b*) where the relaxation time is similar to the time it takes for the metal to flow through the nozzle, $t = l/U \approx 0.055\ s$.

6. CONCLUSIONS

A simple mathematical approach to modeling thixotropic flows has been suggested. The model involves a single transport equation for the apparent viscosity. The steady-state viscosity (at constant shear rate and solid fraction) and the relaxation time can be defined from experimental data. It is shown that it is possible, using this model, to match experimental shear stress hysteresis curves with a reasonable accuracy. However, results for the shear stress appear sensitive to the exact values of the relaxation time. The latter was found to vary significantly for shear rates less than $100\ s^{-1}$. No dependence of the relaxation time on the solid fraction has been investigated.

REFERENCES

1970 S. Richardson, 'The Die Swell Phenomenon,' *Rheological Acta*, Band 9, Heft 2, pp.193-199.

1972 D. P. Spencer, R. Mehrabian, and M. C. Flemings, *Metall. Trans.*, **3**, pp 1925-1932.

1976 P. A. Joly and R. Mehrabian, 'The Rheology of a Partially Solid Alloy,' *Journal of Material Science*, **11**, pp. 1393-1418.

1987 J. M. Sicilian, C. W. Hirt, and R. P. Harper, 'FLOW-3D: Computational Modeling Power for Scientists and Engineers,' *Flow Science, Inc. Report FSI-87-00-01.*

1991 M. C. Flemings, *Metall. Trans.*, **22A**, pp. 957-981.

1993 P. Kumar, C. L. Martin, and S. Brown, 'Shear Rate Thickenning Flow Behavior of Semisolid Slurries,' *Metall. Trans. A*, **24A**, pp. 1107-1116.

1994 D. H. Kirkwood, 'Semisolid Metal Processing,' *International Materials Reviews*, **39**, pp. 173-189.

1995 G. K. Sigworth, 'Rheological Properties of Metal Alloys in the Semi-Solid State,' *Canadian Met. Quart.*, publication pending.

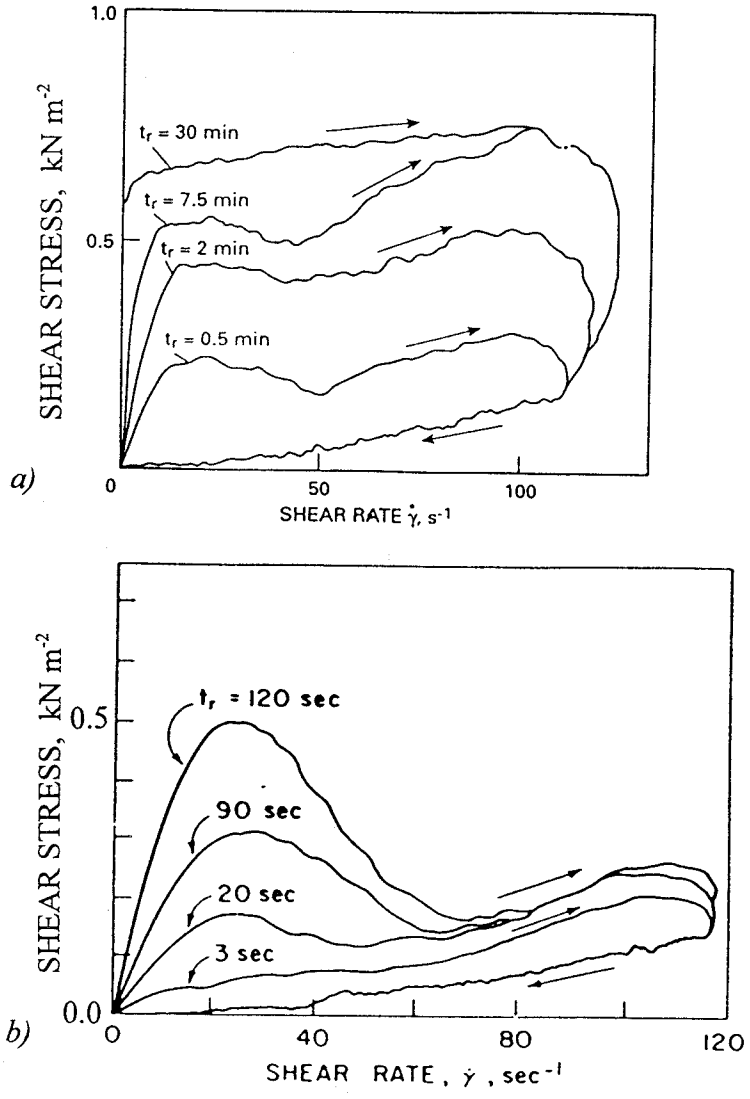

Figure 1. Influence of rest time, t_r, on hysteresis curve for Sn-15%Pb; t_u is the upward time, (*a*) $f_s = 0.45$ and (*b*) $f_s = 0.4$ (after Joly and Mehrabian [1976]).

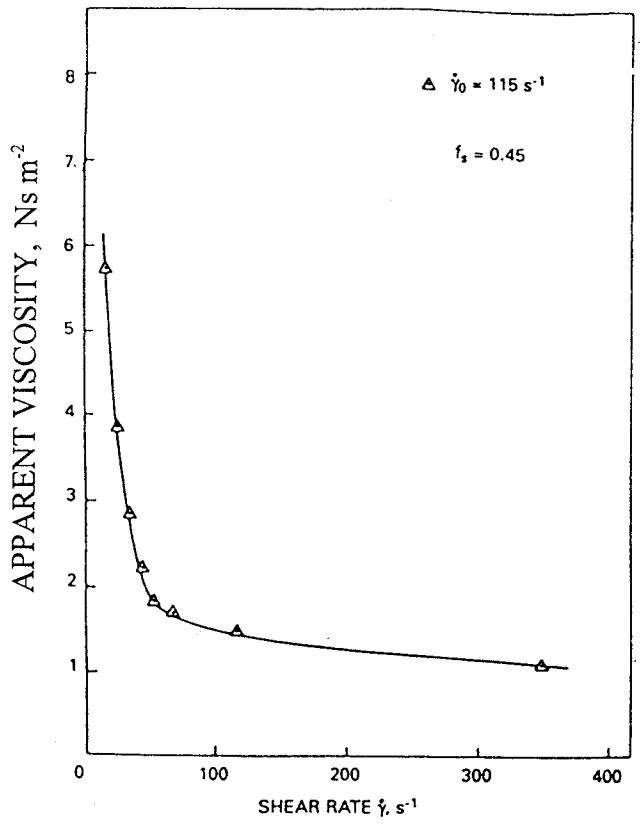

Figure 2. Steady-state viscosity for Sn-15%Pb alloy at $\dot{\gamma} = 115\ s^{-1}$ and $f_s = 0.45$ (after Flemings [1991]).

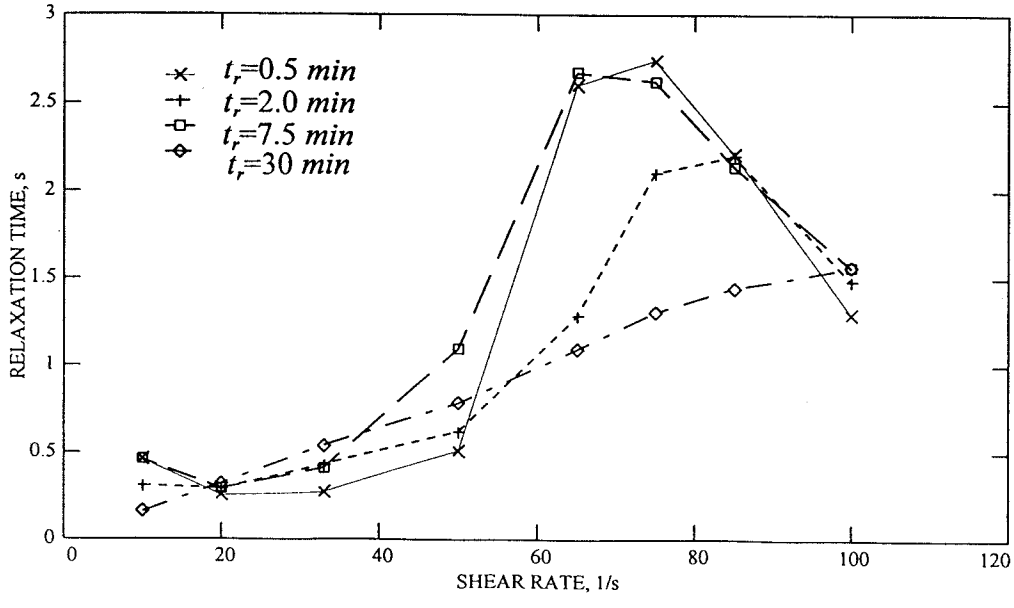

Figure 3. Relaxation time, τ, evaluated from Eq. (7) for different rest times, t_r.

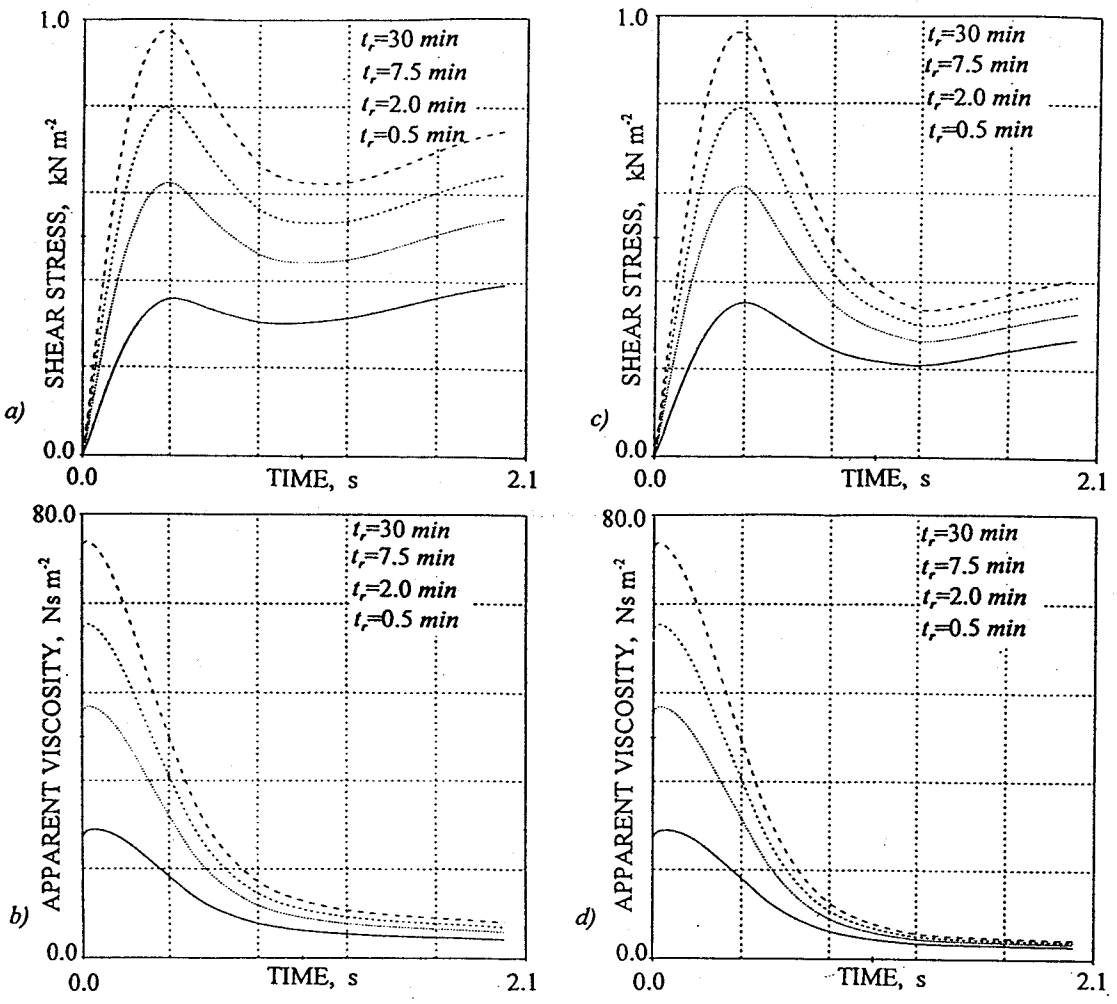

Figure 4. Numerical results: (*a*) and (*b*) shear stress and apparent viscosity computed according to the $\tau_{7.5}$ curve in Fig. 3; (*c*) and (*d*) shear stress and apparent viscosity computed according to the $\tau_{0.5}$ curve in Fig. 3.

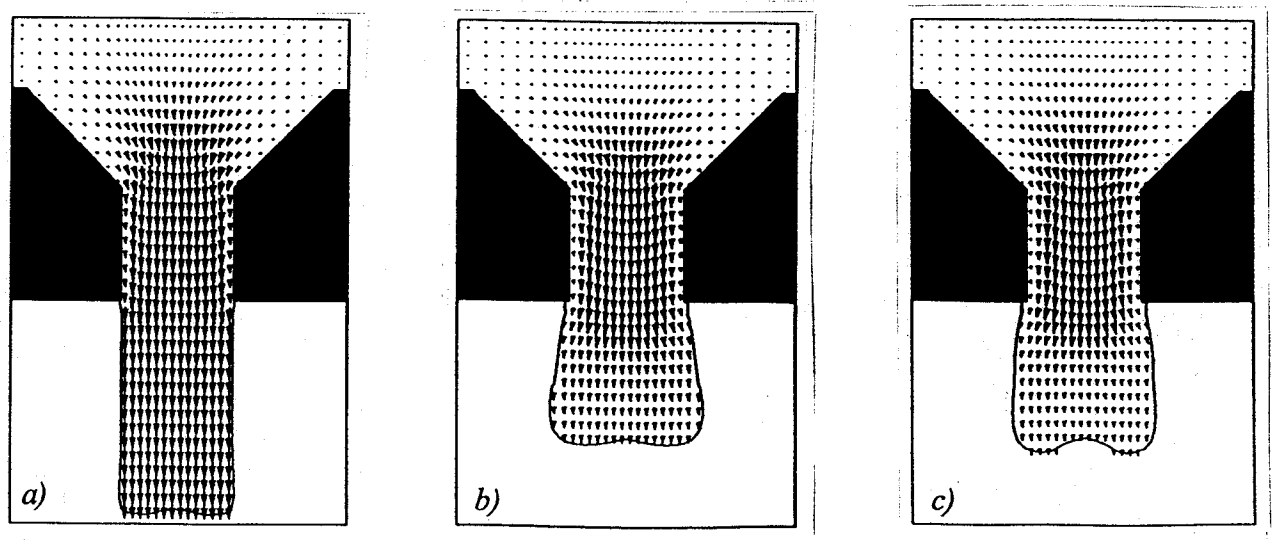

Figure 5. Die swelling during extrusion for a Sn-15%Pb alloy at t=0.16 s: *a*) $\tau = 0.0\ s$, *b*) $\tau = 0.05\ s$ and *c*) $\tau = 10.0\ s$.